sciendo
ISSN 1335-8871
MEASUREMENT SCIENCE REVIEW
Journal homepage: https://content.sciendo.com

Novel Approach to Investigate the Effect of High-Dose Methylprednisolone on Erythrocyte Morphology: White Light Diffraction Microscopy

Cigdem Deniz[1*], Ozlem Kocahan[2], Bengu Altunan[1], Aysun Unal[1]

[1]*Department of Neurology, Tekirdag Namik Kemal University, Tekirdag, Turkey, cdeniz@nku.edu.tr*
[2]*Department of Physics, Tekirdag Namik Kemal University, Tekirdag, Turkey*

Abstract: The present study focuses on quantitative phase imaging of erythrocytes with the aim to evaluate the effects of high-dose methylprednisolone (HDMP) on erythrocytes in vivo under physiological conditions in human blood samples. Samples from ten patients, prescribed to be treated with 1000 mg/day intravenous methylprednisolone for 5 days, were analyzed by white light diffraction phase microscopy (WDPM) for quantitative imaging. WDPM, an optical measurement technique, enables single shot measurement and low speckle noise using white light. Quantitative phase imaging performed with this experimental setup allowed the determination of erythrocyte morphology with 9 different parameters. In vivo quantitative analysis of erythrocytes by WDPM, which is a simple and reliable method, shows that HDMP treatment has no significant effect on erythrocyte morphology. With the developing technology, interdisciplinary studies on individuals under treatment should play an important role in elucidating the interaction between steroids and erythrocytes.

Keywords: Quantitative phase imaging, morphology, erythrocyte, high-dose methylprednisolone, white light diffraction phase microscopy, red blood cell.

1. INTRODUCTION

Drug-induced morphological changes in erythrocytes (red blood cell - RBC) have become a matter of concern among researchers in recent years. Therapeutic drugs such as antiepileptic drugs (carbamazepine, levetiracetam, and others), non-steroidal anti-inflammatory drugs (diclofenac, naproxen, and ibuprofen), the antiviral and antiparkinsonian agent amantadine, beta-blocker labetalol, N-Methyl-D-Aspartate receptor antagonist memantine, and disease-modifying therapies used in MS have been reported to have the potential to affect circulating erythrocytes [1]-[6].

Cell surface research has also recently gained importance in biomedical optical measurement studies. Here, erythrocyte surface observations have generally been performed using scanning electron microscopy (SEM) and atomic force microscopy (AFM) [7]. White light diffraction phase microscopy (WDPM), which is an interferometric technique, enables quantitative measurement of erythrocytes. It is possible to generate quantitative information at the cellular level that can be used to evaluate disease and treatment processes [8]. Structural parameters such as projected surface area (PSA) and mean corpuscular volume (MCV) and mean corpuscular hemoglobin (MCH) can be calculated from the three-dimensional (3D) height profile obtained by quantitative phase imaging (QPI), which is an optical measurement method frequently used in recent years [9]. The WDPM provides quantitative measurement of RBCs, which is an interferometric QPI technique integrating the benefits of both the speed characteristics of off-axis holography and the phase precision related to common-path interferometry [1], [10]-[12]. It allows the determination of RBC morphological parameters without sample preparation and in a non-invasive way. The WDPM, which consists of an interferometer, a light microscope, and a camera, ensures low speckle noise with white light and a single shot measurement [10], [11]. The WDPM allows us to obtain interferometric images. The phase of this interferometric image gives height information. First, a sample interferogram and a reference image without a sample are created, which is used to remove background brightness and noise. Phase information from the sample and reference interferograms is calculated using the preferred phase calculation algorithms. After determining the phase of each point (pixel by pixel) on the sample and the reference surface, the phase of the reference surface is subtracted from the phase of the sample surface to minimize noise. Thus, the sample surface phases obtained for each pixel are combined to generate a 3D surface profile of the sample [13]. The profile generated in this way is quantitative and dynamic, allowing quantitative calculation of morphological parameters related to the sample.

DOI: 10.2478/msr-2023-0026
**Corresponding author: cdeniz@nku.edu.tr (C. Deniz)*

High-dose corticosteroid administration (methyl-prednisolone, 250 to 1000 mg/day, for 3-5 days) has been used since the 1940s to treat inflammatory relapses of autoimmune neurological conditions [14], [15]. High-dose methylprednisolone (HDMP) eliminates acute and chronic inflammation, regardless of the causative agent. Corticosteroids exert their effects at the cellular level through intracellular receptors [16], [17]. The effects of HDMP on inflammation have been examined mainly on lymphocytes, which play an important role in autoimmunity. The changes in platelets and erythrocytes were also found worthy of study by some authors [18]-[20]. Corticosteroids have been reported to form hydrogen bonds with the CO, OH and NH groups of proteins and phospholipids in RBC membranes [20], [21]. While this interaction on the erythrocyte membrane provides therapeutic efficacy, it can also lead to some complications. Hydrophobic interactions can increase the membrane microviscosity by enhancing the compressive elastic stress. This leads to a decrease in the deformability and transport capacity of the erythrocytes. Such erythrocytes act like microthrombi; they clog capillaries and lead to the development of diffusion hypoxia [20], [21].

The effects of steroids on RBC morphology and function have become more interesting and researched, but the results are conflicting and there are still many questions. Previous studies have been performed using experimental in vitro models. The literature still needs in vivo studies with therapeutic doses. Therefore, evaluation of results obtained in vivo under physiological conditions in human blood samples is crucial for understanding the relationship between steroids and erythrocytes. In this study, to clarify the missing part of the steroid-RBC relationship, we investigated the morphological changes of RBCs in individuals receiving therapeutic doses of HDMP using an optical measurement method.

2. MATERIALS AND METHODS

A. Selection of sample

The present study includes ten patients admitted to the Neurology Clinic of our institution with a preliminary diagnosis of demyelinating disease (optic neuritis, neuromyelitis optica, transverse myelitis, multiple sclerosis) and an indication for 5 days of pulse steroid therapy (methylprednisolone 1000 mg/day intravenously (IV)). Patients with co-incidental diseases such as hematologic diseases, diabetes mellitus, renal failure, and soon to be patients using treatment agents and supplementary agents, such as vitamin B12, vitamin D, energy capsules, and others, as well as patients using antiaggregant therapies were not included in the study. Peripheral venous blood samples (2cc) were collected in an ethylenediaminetetraacetic Acid (EDTA) tube on the day before treatment (day 0) and then after the first dose (24 hours), after the third dose (72 hours), after the fifth dose (120 hours), and after 1 month of steroid treatment. Blood was collected primarily in the morning at 06:00 and on an empty stomach. The erythrocytes in all samples were examined using light microscopy (LM) at the time of collection. Five tubes of blood samples obtained from each patient were analyzed by WDPM, and ten RBCs from each blood sample were profiled. Nine parameters related to erythrocyte morphology, namely the height of each pixel h(x,y), mean corpuscular volume (MCV) (μm^3), average cell thickness (ACT) (μm), diameter (D) (μm), projected surface area (PSA) (μm^2), mean corpuscular hemoglobin (MCH) (pico gram), entire cell surface area (SA) (μm^2), circularity (Cr), and sphericity index (SI), were calculated for each profile. Statistical analysis was performed on the obtained data by averaging the parameters in all erythrocytes evaluated for each blood sample.

The permission for the study was granted by the Ethics Committee of Tekirdag Namik Kemal University, Faculty of Medicine (decision number 29.06.2022-176172) and the Institution where the study was conducted. The participating patients were informed about the study and their written consent was obtained stating that they voluntarily participated in the study.

B. Imaging with light microscope

The blood samples were applied to the surface of a glass slide and covered with another slide. Without any further preparation, these sandwiched blood samples were imaged using a Zeiss Axio Observer A1 Inverted microscope with a 40X objective. First, the microscope was adjusted to clarify the image, and the resulting clear light microscope (LM) image of RBCs was captured using a Hamamatsu Orca Flash 4.0 camera.

C. Analysis of the morphological parameters with WDPM

All collected blood samples were prepared for analysis on the day of collection. Samples from the collected blood specimens were applied to the surface of a glass slide and closed with another glass slide. The sandwiched erythrocytes were analyzed using the WDPM setup shown in Fig. 1. The common path interferometer is an interferometer in which the reference beam and the sample beam travel along the same path. Off-axis holography is a setup with a non-zero angle between the reference beam and the sample beam. It requires filtering out spatial frequencies and allows the amplitude and phase information to be obtained with a single image. WDPM is a QPI method that combines the advantages of off-axis holography-specific velocity and phase sensitivity associated with common path interferometry.

Samples are gently placed on the microscope and remain stationary during measurements. An iris is used at the image output port of the Zeiss Axio Observer A1 Inverted microscope to control the output beam diameter. A diffraction grating (110 lp/mm) is placed behind the iris to separate the image field into multiple orders. Diffraction order beams, which carry the exact spatial and phase information, reach the first lens L_1 with a focal length of $f_1 = 60$ mm. The diameter of the diffraction order beam entering lens L_1 is adjusted to 2.6 mm by the iris. In the Fourier plane of L_1, the diffraction pattern is focused on the pinhole, which has two apertures on it. While the zero-order beam passes through a 210 μm aperture, the first-order beam passes through unaffected from the 5 mm aperture. The distance between the two components on the pinhole was measured to be 4 mm. The diameter of the zero-order DC component, which passes through the first

lens, was calculated using the Abbe formula and is $(1.22\lambda f_1/d)$ 15.5 μm, where d = 2.6 mm and λ = 550 nm, which is the center wavelength of the illumination of the microscope. After the pinhole, there is a second lens L_2 with a focal length of 150 mm. The magnification of this system is $M = f_2/f_1 = 2.5$. Through the second lens L_2, the 0 and 1 order beams interfere in the plane of the camera and create an interferogram.

All imaging was performed with a 63x/0.95 objective. The fringe period is measured as 3 pixels per fringe from the interferogram taken with a 63x objective. Hamamatsu ORCA Flash 4.0 CMOS camera was used in the experimental setup. The 2048x2048 pixel image in the camera plane has an effective area of 13,312 mm^2 and a pixel size of 6.5 μm. Considering the 157.5 times magnification value obtained with the interferometer and 63x objective, the size of a pixel in the interferogram was calculated to be 6.5 μm/157.5 = 0.041 μm. Consequently, the red blood cell and the reference plane interferograms were acquired from the WDPM and stored on the computer. Then, these images were processed with Fourier Transform (FT) to determine the phase $\varphi(x, y)$ [12], [13]. Using FT, the phase values for the cell and reference interferograms were retrieved and then subtracted to set the background height value to zero.

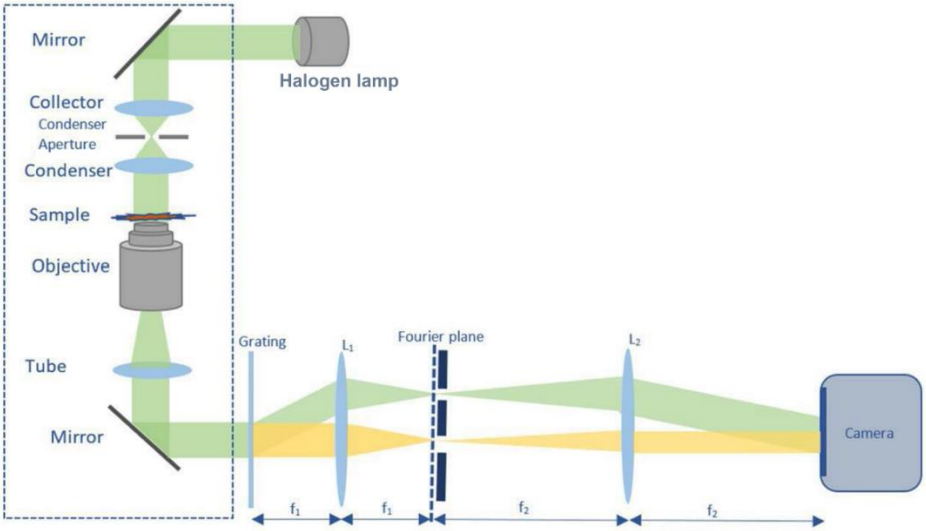

Fig. 1. White light diffraction phase microscopy (WDPM) setup.

Table 1. Morphological parameters calculated for each erythrocyte.

	Parameter Name	Description
1	Height of each pixel h(x,y)	$h(x,y) = \frac{\lambda\varphi(x,y)}{\lvert 2\pi(n_c - n_p)\rvert}$
2	Mean corpuscular volume (MCV)	$MCV = p^2 \sum_{x=1}^{k} \sum_{y=1}^{l} h(x,y)$
3	Average cell thickness (ACT)	$ACT = \frac{\sum_{x=1}^{k} \sum_{y=1}^{l} h(x,y)}{k \times l}$
4	Projected surface area (PSA)	$PSA = Np^2$
5	Mean corpuscular hemoglobin (MCH)	$MCH = \frac{10(OPD_{av})PSA}{\lambda\alpha_{HB}}$
6	Diameter (D)	$D = 2\left(\frac{PSA}{\pi}\right)^{1/2}$
7	Circularity (Cr)	$Cr = \frac{Pr^2}{PSA}$
8	Sphericity (SI)	$SI = \frac{\pi^{1/3}(6MCV)^{2/3}}{SA}$
9	Entire cell surface area (SA)	Determined from the height profile as the sum of all surface areas divided into small triangular pieces

Many parameters can be defined from these phase profiles for the morphological examination of erythrocytes. Table 1 shows the nine morphological parameters and the equations used to calculate them. The phase profiles are converted to height using (1). The wavelength of light used in the microscope is $\lambda = 550$ nm and $n_c = 1.41$ and $n_p = 1.34$ are the refractive index of the cell and the surrounding plasma, respectively [22]. The erythrocyte volume or MCV is calculated using (2) [8], [9]. The ACT can be calculated using (3). One of the morphological parameters is the PSA of the cell in the x-y plane (4) [9], [23], where N is the total number of pixels of the cell in the x-y plane and p is the size of the pixel (0.041 μm). The MCH content can be evaluated using (5) [23], [24], where $\alpha_{HB} = 0.00196$ dl/g is the specific refraction increment, which is mainly related to the protein concentration of hemoglobin. The OPD_{av} is the average optical path difference (OPD) over the projected surface area of the cell. Here, the quantitative phase image in terms of OPD can be expressed as $OPD(x,y) = [\lambda\varphi(x,y)]/2\pi$ [23], which is related to the intracellular refractive index that depends on two factors of cell thickness and the protein and water content of the cells. The D of the cell can be calculated using (6) [9], [23]. The Cr can be defined using (7) as the ratio between the square of the length of the erythrocyte border (Pr) and the PSA. Lastly, the SI is a non-dimensional magnitude between 0 and 1, which was found by (8) [25]. Here, the SA of the RBC is determined from the height profile as the sum of all surface areas being divided into small triangular pieces [25]. In total, nine morphological parameters were calculated from the obtained erythrocyte phase profiles (Table 1). These procedures were performed for ten erythrocytes in each blood sample.

D. Statistical analysis

The statistical package PASW Statistics 25 for Windows was used for data transfer and analysis. Mean, standard deviation, percentage, and expressions were used to express the variables. The normality distribution of the variables was evaluated by the Kolmogorov-Smirnov Test. The Wilcoxon signed-rank test was used to compare those that did not have a normal distribution. A p value of less than 0.05 was considered significant.

3. RESULTS

Five female and five male patients were included in the study. The mean age of all patients was 38.2 ± 8.31 years (female: 41 ± 5.72, male: 35.4 ± 9.47).

We examined all RBCs for their appearance using LM. As in our previously published study on the effects of antiepileptic drugs on erythrocytes, we compared only the morphological changes that may occur visually [1]. To obtain a measurable value, two of the researchers (AU and OK) blindly counted 100 cells manually in the LM images and classified them as biconcave or irregularly shaped. The LM images of the baseline and 72nd h samples are shown in Fig. 2. Although the number of irregular erythrocytes increased in the 72nd h, no significant difference in the number of erythrocytes with irregular morphological features was found in the statistical analysis (Table 2).

By applying FT, the phase distributions were calculated from the interferogram obtained with the WDPM experimental setup and the RBC profiles were obtained in terms of phase $\varphi(x,y)$. Then these phase values were converted to height in μm. Among the RBCs profiled from daily samples, the profiles from the baseline and 72nd h with the diameter value closest to the average diameter value are shown in Fig. 3(a) and Fig. 3(b).

The nine morphological parameters given in Table 1 were calculated from the erythrocyte phase profiles, and the mean values of the parameters are presented in Table 3 together with the time of collection. The mean results of the steroid-free blood samples (Day 0) were compared with the mean results of the blood samples collected after the first, third, and fifth intervals and after the first month, using the Wilcoxon signed-rank test from a non-parametric test. There were no statistical significances between days according to the MCV, ACT, PSA, MCH, D, Cr, SA, and SI of RBCs (Table 4).

Since the purpose of the study was to examine the morphological changes in RBCs related to steroids, the RBC parameters evaluated daily are shown graphically in Fig. 4. At the end of the first month, it was observed that PSA, MCV, MCH, SA, and D showed a decreasing curve compared to the beginning, while ACT, Cr and SI increased (Fig. 4).

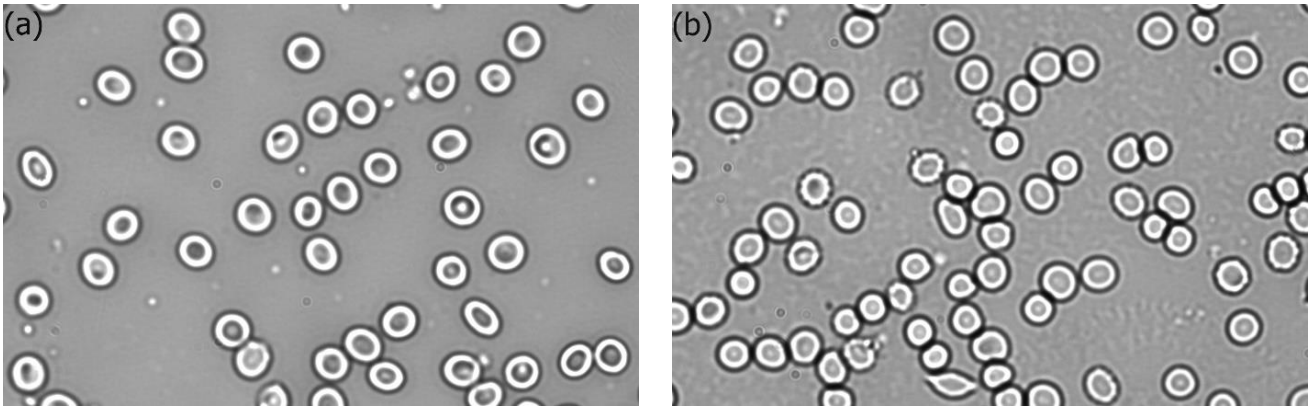

(a) (b)

Fig. 2. Light microscopy (LM) image from (a) 0-day, (b) 72nd h sample for one patient.

Table 2. Irregular erythrocytes calculated with different HDMP exposure times by LM.

Irregular erythrocytes					
	0	24th h	72nd h	20th h	1st month
Mean ± SD (standard deviation)	29.4 ± 11.96	24 ± 14.4	35.1 ± 9.58	21.4 ± 9.09	37.6 ± 16.95
	0-24th h	0-72nd h	0-120th h	0-1st month	
P value	0.41	0.28	0.09	0.60	

†High-dose methylprednisolone (HDMP); ‡ Light microscopy (LM); *p-values <0.05 were considered statistically significant.

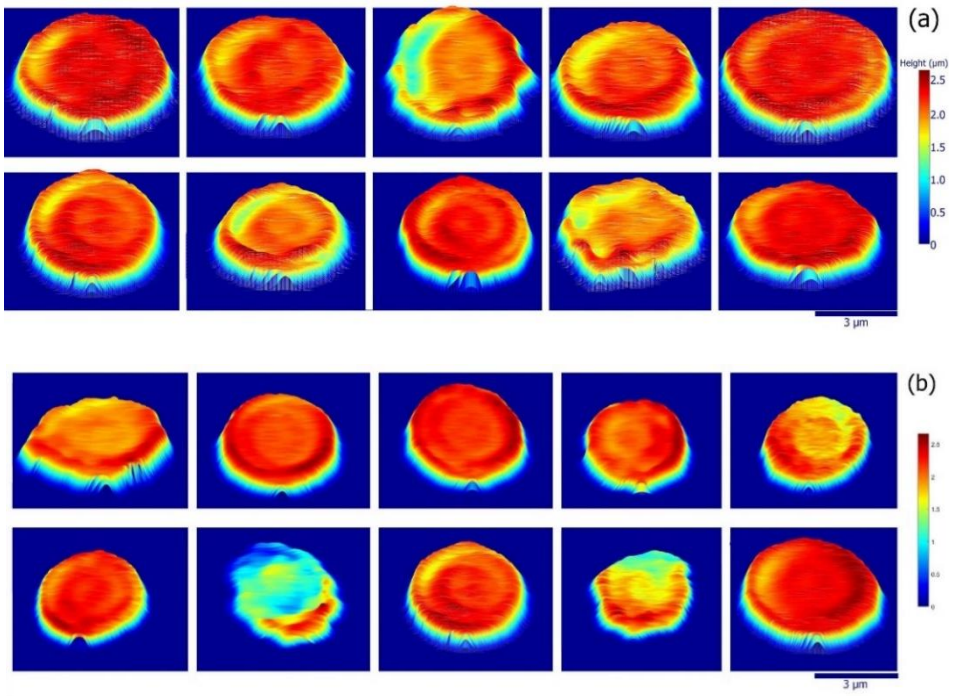

Fig. 3. Red blood cells **(**RBC) height profiles from (a) 0-day, (b) 72nd h samples for each patient with the diameter value closest to the average diameter value.

Table 3. Erythrocyte morphological parameters with different HDMP exposure times by WDPM.

Mean ± SD (standard deviation)					
Parameters	0	24th h	72nd h	120th h	1st month
MCV	93.49 ±17.70	90.11 ±17.22	79.76 ±19.95	96.20 ±15.55	81.03 ±10.22
ACT	1.38 ± 0.11	1.38 ± 0.30	1.26 ± 0.31	1.35 ± 0.14	1.44 ± 0.13
PSA	68.69 ±14.72	66.37 ± 8.98	64.18 ±11.14	72.53 ±16.04	56.56 ± 7.67
MCH	32.07 ± 3.43	32.22 ± 8.13	28.19 ± 6.99	33.03 ± 3.93	31.58 ± 3.21
D	5.24 ± 0.56	5.16 ± 0.34	5.07 ± 0.46	5.38 ± 0.59	4.77 ± 0.33
Cr	0.25 ± 0.03	0.25 ± 0.01	0.26 ± 0.02	0.24 ± 0.03	0.27 ± 0.02
SA	136.41 ±16.33	134.02 ±26.69	127.12 ±26.91	137.31 ±12.39	124.40 ±25.80
SI	0.73 ± 0.10	0.74 ± 0.12	0.72 ± 0.13	0.74 ± 0.08	0.75 ± 0.12

† High-dose methylprednisolone (HDMP); ‡White light diffraction phase microscopy (WDPM); § Mean corpuscular volume (MCV) (μm^3), Average cell thickness (ACT) (µm), Projected surface area (PSA) (μm^2), Mean corpuscular hemoglobin (MCH) (pico gram), Diameter (D) (µm), circularity (Cr), Entire cell surface area (SA) (μm^2), Sphericity Index (SI)

Table 4. Analysis of erythrocyte morphologic parameters with different HDMP exposure times.

P value	0-24th h	0-72nd h	0-120th h	0-1st month
MCV	0.96	0.33	0.39	0.11
ACT	0.76	0.24	0.65	0.18
PSA	0.58	0.65	0.20	0.09
MCH	0.88	0.24	0.33	0.88
D	0.58	0.88	0.20	0.09
Cr	0.67	0.61	0.31	0.11
SA	0.72	0.58	0.96	0.28
SI	0.92	0.44	0.92	0.77

†High-dose methylprednisolone (HDMP); ‡ Mean corpuscular volume (MCV) (μm^3), Average cell thickness (ACT) (μm), Projected surface area (PSA) (μm^2), Mean corpuscular hemoglobin (MCH) (pico gram), Diameter (D) (μm), Circularity (Cr), Entire cell surface area (SA) (μm^2), Sphericity Index (SI); *p-values <0.05 were considered statistically significant.

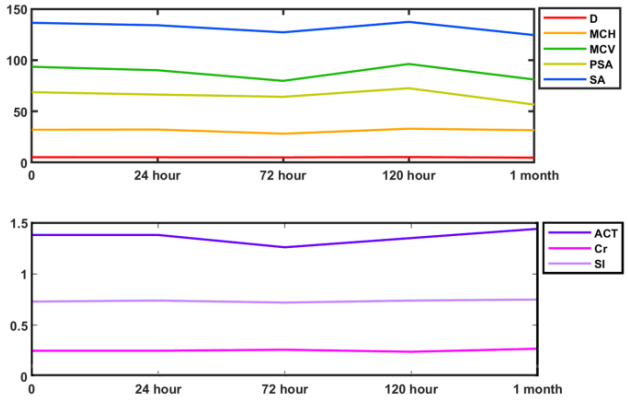

Fig. 4. Erythrocyte morphological parameters changing with different high-dose methylprednisolone (HDMP) exposure times: (a) at the end of the first month, it was observed that projected diameter (D), mean corpuscular hemoglobin (MCH), mean corpuscular volume (MCV), surface area (PSA) and the entire cell surface area (SA) show a decreasing curve compared to the baseline; (b) at the end of the first month, it was observed that the average cell thickness (ACT), circularity (Cr) and sphericity ındex (SI) show an increasing curve compared to the baseline.

4. Discussion

The aim of this study was to quantitatively analyze the relationship between the RBC morphological properties and HDMP exposure time. In contrast to the few studies reported in the literature, our in vivo analyses revealed that HDMP treatment did not significantly alter RBC morphology (Table 3 and Table 4). Zuk et al. (2011) studied the effects of methylprednisolone on RBCs of asthma patients. They found that the stiffness of RBCs incubated with high concentrations of methylprednisolone increased with incubation time, and RBC morphology changed significantly. They also reported that similar effects were not observed at lower concentrations. The authors concluded that the efficiency of high-dose steroids used in clinical practice to open bronchial arteries may be low [26]. The reason why we did not reach similar results may be that the authors performed the morphological assessments on RBCs under in vitro conditions. From a clinical point of view, the effects of therapeutic blood steroid levels achieved by high-dose steroid therapy on RBCs may be different from direct incubation.

Recent studies strongly demonstrate the contribution of RBCs to both hemostasis and thrombosis, including their key role in venous thrombo-embolism (VTE) and clot contraction processes [27], [28]. Corticosteroids are used in low dose (<7.5 mg/day), medium dose (>7.5 mg – 30 mg/day), high dose (30 mg – 100 mg/day) and very high dose (>100 mg/day) depending on the diagnosis and clinical experience [15]. It has been reported that the use of prednisone at doses higher than 20 mg and for prolonged periods increases the risk of both arterial and venous thrombosis more than other risk factors [29]. Therefore, in this study, we were also motivated to investigate whether HDMP treatment could increase susceptibility to venous thrombosis by morphologically altering RBCs. Although our results do not support the studies highlighting that methylprednisolone causes a significant change in erythrocyte stiffness and morphology depending on drug concentration and incubation time [26], they are in line with the findings of Go et al. (2022) [30]. Go et al. reported that a high-dose MP was not associated with a higher risk of VTE compared with a low dose MP [30]. When interpreting these results, it is important to keep in mind that thrombosis development is multifactorial and vascular morphology may also influence the thrombotic potential associated with steroids [28]. Nevertheless, we believe that our results are important to guide future studies aimed at explaining the lower incidence of venous thrombosis in short-term HDMP treatment compared with long-term low-dose. Further studies with different doses, durations, and disease groups investigating the effects of steroids on erythrocytes would be pharmacologically useful to explain many unknown points of the mechanisms of action of methylprednisolone.

One of the strong aspects of this study is that we conducted this research using a method that has been shown to be reliable. When we compared the data obtained in this study with the data obtained in our previous study, in which we examined the effect of antiepileptic drugs, we found that antiepileptic-induced RBC morphological changes did not develop during HDMP treatment [1]. Analyzing the graphs of parameters calculated by WDPM, it was found that SA, MCV, MCH and D showed a decreasing curve at the end of the first month compared with the beginning, while ACT, Cr and SI increased (Fig. 4). In light microscopy (Fig. 2) and WDPM (Table 4) examinations, although slight changes in

numerical parameters associated with deterioration in erythrocyte morphology were observed at 72nd hour, no statistically significant change was observed. Jaferzadeh and Moon [9] classified erythrocyte morphological appearances using morphological parameter values in 3D imaging. According to this classification, we observed that the changes in MCV, MCH, ACT and D values were within the normal range defined for biconcave erythrocytes, but SA increased. The biconcave shape is important for the functionality of RBCs, as they can transform into ellipsoidal structures at high shear rates [31]. It allows the membrane to have a high surface-to-volume ratio, which facilitates large reversible elastic deformation of the RBC without compression when passing through small capillaries [32]-[34]. The average SA values of RBCs in the 1st month in our study were compatible with the values of echinospherocyte shape. Together with the slight changes described above, which did not reach statistical significance in the early period, this result suggests that there may be long-term morphological changes that begin with the change in SA.

The main limitation of this study is that we did not evaluate parameters related to the functional properties of erythrocytes (membrane structure and internal viscosity) and did not perform erythrocyte typing. We reliably found no changes in erythrocyte morphology with short-term high-dose use, but the evaluation period may not have been long enough to detect changes. The patient population and the sample size may also affect the results. Therefore, our findings should be supported by further studies with other patient groups and a larger number of cases.

5. Conclusion

In conclusion, quantitative in vivo analysis of RBCs by WDPM, which is a simple and reliable optical measurement method, shows that the HDMP treatment does not significantly alter erythrocyte morphology. However, because of the presence of graphical and numerical changes that did not reach statistical significance in light microscopy and WDPM examinations, studies of longer duration, with a larger number of cases, and involving different patient groups are needed. With the developing technology, interdisciplinary studies with individuals under treatment should play an important role in elucidating the interaction between steroids and RBCs.

Acknowledgment

This work is supported by the Turkish Scientific and Technical Research Council. Grant number: 122E201.

Abbreviations

ACT: Average Cell Thickness, AFM: Atomic Force Microscopy, Cr: Circularity, D: Diameter, EDTA Ethylenediaminetetraacetic Acid, FT: Fourier Transform, HDMP: High Dose Methylprednisolone, IV: Intravenous, LM: Light Microscopy, MCH: Mean Corpuscular Hemoglobin, MCV: Mean Corpuscular Volume, OPD: Optical Path Difference, PSA: Projected Surface Area, QPI: Quantitative Phase Imaging, RBC: Red Blood Cell, SA: Entire Cell Surface Area, SEM: Scanning Electron Microscopy, SI: Sphericity Index, VTE: Venous Thromboembolic Events, WDPM: White Light Diffraction Phase Microscopy, 3D: Three-dimensional

References

[1] Unal, A., Kocahan, O., Altunan, B., Gundogdu, A. A., Uyanık, M., Ozder, S. (2021). Quantitative phase imaging of erythrocyte in epilepsy patients. *Microscopy Research and Technique*, 84 (6), 1172-1180. https://doi.org/10.1002/jemt.23676

[2] Zambrano, P., Suwalsky, M., Jemiola-Rzeminska, M., Strzalka, K. (2018). α1-and β-adrenergic antagonist labetalol induces morphological changes in human erythrocytes. *Biochemical and Biophysical Research Communications*, 503 (1), 209-214. https://doi.org/10.1016/j.bbrc.2018.06.004

[3] Zambrano, P., Suwalsky, M., Villena, F., Jemiola-Rzeminska, M., Strzalka, K. (2017). In vitro effects of the anti-Alzheimer drug memantine on the human erythrocyte membrane and molecular models. *Biochemical and Biophysical Research Communications*, 483 (1), 528-533. https://doi.org/10.1016/j.bbrc.2016.12.111

[4] Suwalsky, M., Jemiola-Rzeminska, M., Altamirano, M., Villena, F., Dukes, N., Strzalka, K. (2015). Interactions of the antiviral and antiparkinson agent amantadine with lipid membranes and human erythrocytes. *Biophysical Chemistry*, 202, 13-20. https://doi.org/10.1016/j.bpc.2015.04.002

[5] Lieser, J., Schwedes, C., Walter, M., Langenstein, J., Moritz, A., Bauer, N. (2021). Oxidative damage of canine erythrocytes after treatment with non-steroidal anti-inflammatory drugs. *Tierärztliche Praxis*, 49 (6), 407-413. https://doi.org/10.1055/a-1623-7506

[6] Groen, K., Maltby, V. E., Sanders, K. A., Scott, R. J., Tajouri, L., Lechner-Scott, J. (2016). Erythrocytes in multiple sclerosis - forgotten contributors to the pathophysiology? *Multiple Sclerosis Journal - Experimental Translational and Clinical*. https://doi.org/10.1177/2055217316649981

[7] Mukherjee, R., Saha, M., Routray, A., Chakraborty, C. (2015). Nanoscale surface characterization of human erythrocytes by atomic force microscopy: A critical review. *IEEE Transactions Nanobioscience*, 14 (6), 625-33. https://doi.org/10.1109/TNB.2015.2424674

[8] Ahmadzadeh, E., Jaferzadeh, K., Lee, J., Moon I. (2017). Automated three-dimensional morphology-based clustering of human erythrocytes with regular shapes: Stomatocytes, discocytes, and echinocytes. *Journal of Biomedical Optics*, 22 (7), 076015. https://doi.org/10.1117/1.JBO.22.7.076015

[9] Jaferzadeh, K., Moon, I. (2016). Human red blood cell recognition enhancement with three-dimensional morphological features obtained by digital holographic imaging. *Journal of Biomedical Optics*, 21 (12), 126015. https://doi.org/10.1117/1.JBO.21.12.126015

[10] Bhaduri, B., Pham, H., Mir, M., Popescu, G. (2012). Diffraction phase microscopy with white light. *Optic Letters*, 37 (6), 1094-1096. https://doi.org/10.1364/ol.37.001094

[11] Pham, H. V., Edwards, C., Goddard, L. L., Popescu, G. (2013). Fast phase reconstruction in white light diffraction phase microscopy. *Applied Optics*, 52 (1), A97-A101. https://doi.org/10.1364/ao.52.000a97

[12] Kocahan, O., Tiryaki, E., Coskun, E., Ozder, S. (2018). Determination of phase from the ridge of CWT using generalized Morse wavelet. *Measurement Science And Technology*, 29 (3), 035203. https://doi.org/10.1088/1361-6501/aa9d56

[13] Takeda, M., Mutoh, K. (1983). Fourier transform profilometry for the automatic measurement of 3-D object shapes. *Applied Optics*, 22 (24), 3977. https://doi.org/10.1364/ao.22.003977

[14] Bayazit, S., Engin, B., Kutlubay, Z., Aşkın, O., Serdaroglu S. (2020). Side effects of systemic steroids and management. *Dermatoz,* 11 (1), 1-6. https://doi.org/10.4274/dermatoz.galenos.2019.76486

[15] Buttgereit, F., da Silva, J. A., Boers, M., Burmester, G. R., Cutolo, M., Jacobs, J., Kirwan, J., Köhler, L., Van Riel, P., Vischer, T., Bijlsma, J. W. (2002). Standardised nomenclature for glucocorticoid dosages and glucocorticoid treatment regimens: Current questions and tentative answers in rheumatology. *Annals of the Rheumatıc Diseases*, 61 (8), 718-722. https://doi.org/10.1136/ard.61.8.718

[16] McGowan Jr., J. E., Chesney, P. J., Crossley, K. B., LaForce, F. M. (1992). Guidelines for the use of systemic glucocorticosteroids in the management of selected infections. *The Journal of Infectious Diseases*, 165 (1), 1-13. https://doi.org/10.1093/infdis/165.1.1

[17] Van Der Meer, J. W. (2003). Immunomodulation by antimicrobial drugs. *Netherlands Journal of Medicine*, 61 (7), 233-234.

[18] Shimba, A., Ikuta, K. (2020). Control of immunity by glucocorticoids in health and disease. *Seminars in Immunopathology*, 42 (6), 669-680. https://doi.org/10.1007/s00281-020-00827-8

[19] Thomason, J., Mooney, A. P., Price, J. M., Whittemore, J. C. (2020). Effects of clopidogrel and prednisone on platelet function in healthy dogs. *Journal of Veterinary Internal Medicine*, 34 (3), 1198-1205. https://doi.org/10.1111/jvim.15759

[20] Panin, L. E., Mokrushnikov, P. V., Kunitsyn, V. G., Zaitsev, B. N. (2010). Interaction mechanism of cortisol and catecholamines with structural components of erythrocyte membranes. *Journal of Physical Chemistry B*, 114 (29), 9462-9473. https://doi.org/10.1021/jp911917a

[21] Mokrushnikov, P. V., Panin, L. E., Zaitsev, B. N. (2015). The action of stress hormones on the structure and function of erythrocyte membrane. *General Physiology and Biophysics*, 34 (3), 311-321. https://doi.org/10.4149/gpb_2014041

[22] Popescu, G., Badizadegan, K., Dasari, R. R., Feld, M. S. (2006). Observation of dynamic subdomains in red blood cells. *Journal of Biomedical Optics*, 11 (4), 040503. https://doi.org/10.1117/1.2221867

[23] Jaferzadeh, K., Sim, M., Kim, N., Moon, I. (2019). Quantitative analysis of three-dimensional morphology and membrane dynamics of red blood cells during temperature elevation. *Scientific Reports*, 9 (1), 14062. https://doi.org/10.1038/s41598-019-50640-z

[24] Yi, F., Moon, I., Javidi, B. (2016). Cell morphology-based classification of red blood cells using holographic imaging informatics. *Biomedical Optics Express*, 7 (6), 2385-2399. https://doi.org/10.1364/boe.7.002385

[25] Park, H., Lee, S., Ji, M., Kim, K., Son, Y., Jang, S., Park, Y. (2016). Measuring cell surface area and deformability of individual human red blood cells over blood storage using quantitative phase imaging. *Scientific Reports*, 6, 34257. https://doi.org/10.1038/srep34257

[26] Zuk, A., Targosz-Korecka, M., Szymonski, M. (2011). Effect of selected drugs used in asthma treatment on morphology and elastic properties of red blood cells. *International Journal of Nanomedicine*, 6, 249-257. https://doi.org/10.2147/ijn.s15802

[27] Byrnes, J. R., Wolberg, A. S. (2017). Red blood cells in thrombosis. *Blood*, 130 (16), 1795-1799. https://doi.org/10.1182/blood-2017-03-745349

[28] Weisel, J. W., Litvinov, R. I. (2019). Red blood cells: The forgotten player in hemostasis and thrombosis. *Journal of Thrombosis and Haemostasis*, 17 (2), 271-282. https://doi.org/10.1111/jth.14360

[29] Hickman, K., Magder, L., Petri, M. (2015). Prednisone increases both arterial and venous thrombosis in SLE. *Annals of the Rheumatic Diseases*, 74, 573. https://doi.org/10.1136/annrheumdis-2015-eular.4276

[30] Go, R. C., Nyirenda, T., Bojarian, M., Hosseini, D. K., Rahim, M., Kim, K., Rose, K. M. (2022). Methylprednisolone, venous thromboembolism, and association with heparin to 30 days in hospital survival in severe Covid-19 pneumonia. *BMC Pulmonary Medicine*, 22, 6. https://doi.org/10.1186/s12890-021-01810-1

[31] Baskurt, O. K., Meiselman, H. J. (2003). Blood rheology and hemodynamics. *Seminars in Thrombosis and Hemostasis*, 29 (5), 435-450. https://doi.org/10.1055/s-2003-44551

[32] Canham, P. B. (1970). The minimum energy of bending as a possible explanation of the biconcave shape of the human red blood cell. *Journal of Theoretical Biology*, 26 (1), 61-81. https://doi.org/10.1016/s0022-5193(70)80032-7

[33] Uzoigwe, C. (2006). The human erythrocyte has developed the biconcave disc shape to optimise the flow properties of the blood in the large vessels. *Medical Hypotheses*, 67 (5), 1159-1163. https://doi.org/10.1016/j.mehy.2004.11.047

[34] Tu, Z. (2011). Geometry of membranes. *Journal of Geometry and Symmetry in Physics*, 24, 45-75. https://doi.org/10.7546/jgsp-24-2011-45-75

Received March 29, 2023
Accepted September 18, 2023